A Study on Sliding Mode Observer Design for Robust State Estimation during Load Follow **Operation**

Dongju Choi a and Yonghee Kim a* ^aDepartment of Nuclear and Quantum Engineering, KAIST *Corresponding author: yongheekim@kaist.ac.kr

*Keywords: Sliding Mode Observer, Chattering Phenomenon, Adaptive Gain, Load Follow Operation

1. Introduction

Since xenon concentration in a nuclear reactor system cannot be directly measured, estimating its change during power variations is a major challenge in load follow operations. Sliding Mode Observer (SMO) has been introduced to estimate the xenon concentration [1].

Sliding Mode Theory is a widely used nonlinear control technique based on the principle of variable structure systems. Its core strategy is to define a sliding surface in the state-space and design a discontinuous control action that drives the system's state trajectory onto this surface. Once on the surface, the system enters a sliding mode, where its dynamics become insensitive to a class of disturbances.

One of the critical issues in Sliding Mode Theory is chattering, an undesirable oscillation with finite frequency and amplitude. Chattering on sliding surface destabilizes the estimation dynamics and reduces control accuracy. In digital implementations, it often manifests as discretization chattering caused by the finite sampling rates.

This study aims to design a sliding mode observer that effectively mitigates chattering phenomenon and ensures robust state estimation under disturbances. The implicit Euler method is employed to mitigate numerical chattering, and an adaptive gain law is developed for both the observer and the controller to ensure stable estimation and accurate trajectory tracking, respectively.

2. Preliminary

2.1. Reactor Core Model

The reactor core model for the observer consists of the point kinetics and xenon-iodine balance equations, as shown ins Eqs. (1) - (4). This model is coupled with a lumped heat balance model Eqs. (5) - (7) and a reactivity feedback model Eqs. (8) - (9).

$$\dot{p} = \frac{\rho - \beta}{\Lambda} + \sum_{i=1}^{G_d} \lambda_i C_i, \qquad i = 1, 2, \dots, G_d$$
 (1)

$$\dot{C} = \frac{\beta_i}{\Lambda} p - \lambda_i C_i$$

$$\dot{I} = \gamma_I \Sigma_f \phi - \lambda_I I$$

$$\dot{X} = \gamma_X \Sigma_f \phi + \lambda_I I - \sigma_a^X X \phi - \gamma_X X$$
(4)

$$\dot{I} = \gamma_I \Sigma_f \phi - \lambda_I I \tag{3}$$

$$\dot{X} = \gamma_x \Sigma_f \phi + \lambda_I I - \sigma_a^X X \phi - \gamma_x X \tag{4}$$

$$M_f c_f \dot{T}_f = P(t) - \frac{T_f(t) - T_{cl}(t)}{R_g}$$
 (5)

$$M_{cl}c_{cl}\dot{T}_{cl} = \frac{T_f(t) - T_{cl}(t)}{R_a} - \frac{T_{cl}(t) - T_c(t)}{R_c}$$
(6)

$$M_{f}c_{f}\dot{T}_{f} = P(t) - \frac{T_{f}(t) - T_{cl}(t)}{R_{g}}$$
(5)

$$M_{cl}c_{cl}\dot{T}_{cl} = \frac{T_{f}(t) - T_{cl}(t)}{R_{g}} - \frac{T_{cl}(t) - T_{c}(t)}{R_{c}}$$
(6)

$$M_{c}c_{c}\dot{T}_{c} = \frac{T_{cl}(t) - T_{c}(t)}{R_{c}} - 2w(t)c_{c}[T_{c}(t) - T_{in}(t)]$$
(7)

$$\rho = \rho_r + \alpha_f (T_f - T_{f0}) + \alpha_c (T_c - T_{c_0})$$

$$-\frac{\sigma_a^X (X - X_0)}{\nu \Sigma_f}$$
(8)

$$\dot{\rho} = G_r Z_r \tag{9}$$

Table 1. System parameter values used in the SMO

Parameter	Value	Parameter	Value
Λ (sec)	2E-5	c _{cl} (J/kg.K)	330
V (cm ³)	1E+7	c _c (J/kg.K)	6748
γ_X	2.8508E-3	M _f (kg)	65722
γ_I	6.3482E-2	M _{cl} (kg)	13539
$\lambda_X(\text{sec}^{-1})$	2.1E-5	M_c (kg)	151456
$\lambda_I (\text{sec}^{-1})$	2.9E-5	w (kg/sec)	10516
$R_g(\text{sec.}\mathbb{C}/\mathbb{J})$	1.3E-7	$\alpha_f (\Delta k/k/^{\circ}C)$	-3.24E-05
$R_c(\text{sec.}C/J)$	2.64E-8	$\alpha_c (\Delta k/k/^{\circ}C)$	-2.13E-04
c_f (J/kg.K)	247	G _r (pcm)	14.5E-3

where G_r is total reactivity worth of the control rod and Z_r is the control rod speed, which is the control input for the controller. All other notations follow standard conventions.

2.2. Sliding Mode Theory

Sliding Mode Control is a type of variable structure control system in which the system dynamics are forced to reach and stay on a predefined sliding surface. The motion along this surface is determined by a feedback control law and a switching rule.

Let a general non-linear system be expressed as

$$\dot{x} = f(x) + g(x)u$$

$$y = h(x)$$
(10)

where u is a control input for controller, and f, g, and hare sufficiently smooth functions.

Then, the sliding surface is defined as

$$s(t) = \left(m + \frac{d}{dt}\right)^{r-1} e(t) \tag{11}$$

where e(t) is an error between the measurable state and its desired value, r is a relative degree and m is a strictly positive constant.

From the η reachability law of the attractive equation, the dynamics of sliding surface is also defined as

$$\dot{s} = -\eta \tanh\left(\frac{s}{\varphi}\right) \tag{12}$$

where η is another gain for the sliding mode control.

The hidden state x(t) may not be directly measured, thus an observer is designed, and the observed states is used for feedback control. Considering the non-linear system described in Eq (13). The corresponding sliding mode observer is defined in Eq (14).

$$\dot{x} = f(x, u, t)
y = g(x, u, t)$$
(13)

$$\dot{\hat{x}} = f(\hat{x}, u, t) + k(y - \hat{y}) + \psi \tanh\left(\frac{y - \hat{y}}{\varphi}\right)
\hat{y} = g(\hat{x}, u, t)$$
(14)

where x represents a state vector, y is measurable output, \hat{x} is the estimated state vector, and f and g are non-linear function representing the system dynamics. The parameters k and ψ denote the observer gain, and φ is a deadband width introduced to avoid frequent switching. In the reactor core system, the state vector \hat{x} is expressed as

$$\hat{x} = \left[\hat{p}, \hat{C}_1, \dots, \hat{C}_{Gd}, \hat{I}, \hat{X}\right]^T \tag{15}$$

2.3. Stability analysis of the designed sliding mode observer system.

In order to prove that the sliding mode observer can provide convergent state observation, Lyapunov stability analysis can be used. Using the estimation error of states, consider the Lyapunov-function candidate,

$$V = \frac{1}{2} \left(e_p^2 + \sum_{i=1}^{G_d} e_{C_i}^2 + e_I^2 + e_X^2 \right)$$
 (16)

where

$$\begin{cases} e_p = p - \hat{p} \\ e_{C_i} = C_i - \hat{C}_i \\ e_I = I - \hat{I} \\ e_X = X - \hat{X} \end{cases}$$
 (17)

And its derivative is expressed as follows,

$$\dot{V} = e_p \dot{e}_p + \sum_{i=1}^{G_d} e_{C_i} \dot{e}_{C_i} + e_I \dot{e}_I + e_X \dot{e}_X$$
 (18)

Therefore, by ensuring that \dot{V} is negative definite, the observer gains can be determined.

3. Methodology

3.1. Implementation of Implicit Euler Method

The selection of numerical integration scheme plays a crucial role in the discretization of sliding mode systems. The explicit Euler method is straightforward to implement but often amplifies discretization chattering, since the control update is delayed with respect to the state evolution. The implicit Euler method, by contrast, mitigates discretization chattering through its inherent numerical structure.

Applying the implicit Euler scheme to the observer dynamics leads to a nonlinear algebraic equation of the form

$$x_{k+1} = x_k + \Delta t f(x_{k+1})$$

$$x = [p, C_1, \dots, C_{G_d}, I, X]^{\mathrm{T}} \in \mathbb{R}^{G_d + 3}$$
(19)

Since the resulting equation cannot be solved analytically, the state at each step is obtained numerically using the Newton-Raphson method.

3.2. Adaptation law for adaptive gain

Control performance is critically influenced by how system gains are designed. Fixed-gain approaches may work under limited operating conditions but often degrade in the presence of variations or disturbances. Adaptive gain mechanisms overcome this issue by adjusting in real time according to system states, thereby maintaining reliable operation. In the proposed observer framework, both the sliding gain $\hat{\eta}$ and the observer gains are adaptively updated through Lyapunov-based laws.

Considering the Lyapunov function candidate for adaptive law,

$$V = \frac{1}{2} \left(s^2 + \frac{1}{\gamma_{\eta}} e_{\eta}^2 \right) \tag{20}$$

where e_{η} is an error between adaptive gain $\hat{\eta}$ and ideal gain η^* , γ_{η} is a adaptive rate. To gaurantee the negative definite of \dot{V} , the adaptation law of $\hat{\eta}$ is derived as:

$$\dot{\hat{\eta}} = \gamma_{\eta} s \tanh\left(\frac{s}{\omega}\right) \tag{21}$$

In the same way, the adaptation law for the adaptive observer gains \hat{k}_1 and $\hat{\psi}_1$ are derived as follows:

$$V = \frac{1}{2} \left(e_p^2 + \sum_{i=1}^{G_d} e_{C_i}^2 + e_i^2 + e_X^2 + \frac{1}{\gamma_{k_1}} e_{k_1}^2 + \frac{1}{\gamma_{\psi_1}} e_{\psi_1}^2 \right)$$
(22)

$$\dot{k}_1 = \gamma_{k_1} e_p \tag{23}$$

$$\dot{\psi}_1 = \gamma_{\psi_1} e_p \tanh\left(\frac{e_p}{\omega}\right) \tag{24}$$

$$\dot{\hat{\psi}}_1 = \gamma_{\psi_1} e_p \tanh\left(\frac{e_p}{\omega}\right) \tag{24}$$

where e_{k_1} and e_{ψ_1} denote the estimation errors between the adaptive observer gains and their ideal values, while $\gamma_{k_1}, \gamma_{\psi_1}$ are the corresponding adaptation rates. It should be emphasized that the observer model involves multiple gain parameters, but the adaptive law is applied only to the first gains, since they are directly related to the dominant system dynamics.

4. Results

4.1. Load Follow Operation

Simulations are performed for the standard APR1400 core at beginning of cycle conditions using the KANT reactor core simulator, a 3-D diffusion nodal code [2]. A 24-hour DLFO is considered, and the power signal provided to the observer is perturbed by $\pm 3\%$ to model external disturbances. The overall simulation scheme is illustrated in the Figure 1. For the load follow operation, SMO module will be continuously invoked during the time-dependent neutronic/TH coupled solution. During the simulation, the control rod positions are adjusted based on the Mode-K+ control logic to follow the demand power, and the resulting reactor power is fed into the SMO for state estimation.

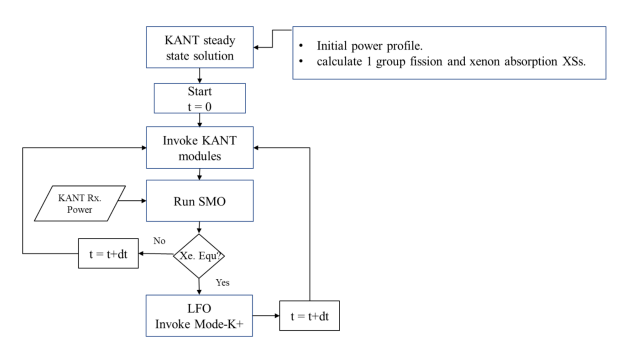


Figure 1. SMO-assisted DLFO implementation flowchart.

Figure 2 shows the xenon estimation performance of the proposed implicit SMO during DLFO simulation. The results are compared against the reference solution obtained from the KANT reactor model. As shown in the top plot, the estimated xenon concentration closely tracks the KANT reference solution throughout the entire transient. As detailed in the bottom plot, the relative estimation error remains below 3.5%, confirming the high accuracy and reliability of the proposed observer.

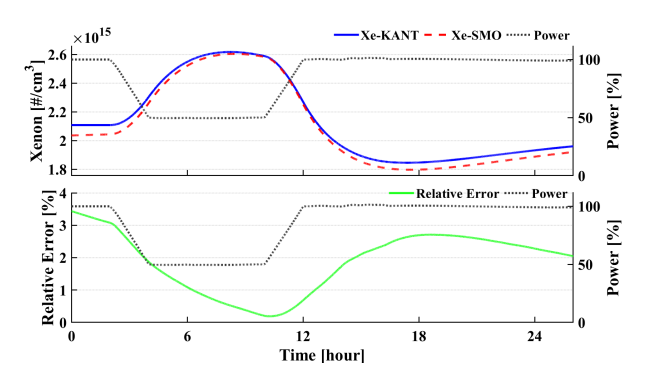


Figure 2. Xenon estimation during 24-hour Load Follow Operation

4.2. Comparison of Explicit and Implicit SMO

Figure 3 illustrates the distinct performance difference between the conventional Explicit SMO and the proposed Implicit SMO. The estimated power from the Explicit SMO exhibits significant high-frequency oscillations (chattering), whereas the Implicit SMO produces a relatively smooth and stable signal.

Table 1 quantifies this comparison. To achieve an estimation error of $\pm 0.5\%$, the Explicit SMO required a time step of 1E-5 seconds, resulting in an execution time of 2292 seconds. The Implicit SMO achieved the same error level with a 10,000 times larger time step of 0.1 s, and the corresponding execution time was approximately 600 times shorter. For the Implicit SMO, increasing the time step from 0.1 s to 1.0 s increased the estimation error from $\pm 0.5\%$ to $\pm 1.0\%$.

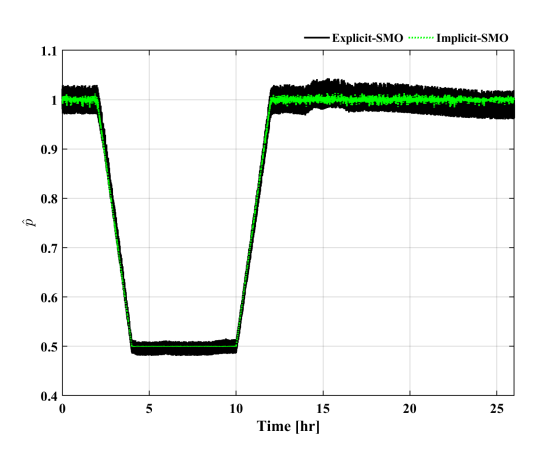


Figure 3. Estimated power using explicit and implicit SMO

Table 1. Performance Comparison of Explicit and Implicit SMO

	Time step (sec)	Execution Time (sec)	Maximum Relative Error in Power Estimation (%)
Explicit	1E-5	2292	0.5%
	5E-5	394	5.0%
Implicit	0.1	3.8	-
	0.5	4.3	0.5%
	1.0	9.5	1.0%

4.3. Performance of Adaptive Gain Observer

The parameters and gains of an observer are typically tuned and determined for a specific nominal operating point, which is often the full-power steady-state condition. However, during a load-follow operation, the reactor power and internal system dynamics change significantly. Consequently, the performance of an observer with gains fixed for full-power conditions is expected to degrade when the reactor operates at different power levels. This performance degradation is demonstrated in Figure 3, where the estimation accuracy for the fixed-gain case clearly differs between the 50% and 100% power intervals.

Figure 4 presents the estimated states and their relative errors under adaptive gain implementation. The results show that the adaptive SMO effectively mitigates chattering across different power conditions, thereby providing stable estimation of power states. Unlike the fixed-gain case, the adaptive method dynamically adjusts the observer gain in response to external disturbances and varying power levels, ensuring robustness of the estimation process.

It is noteworthy that the relative errors for the xenon and iodine estimations appear significantly smaller and smoother than the error in the power estimation. This is attributed to the inherently slow dynamics of xenon and iodine, which naturally filter the high-frequency chattering present in the power estimation. However, the stability of the power estimation is critical, as it serves as the foundation for the entire observer system. Any instability or sustained chattering in this primary estimate will eventually propagate and corrupt all other state estimations.

The evolution of adaptive gains is shown in Figure 5. The variation of these gains highlights their ability to compensate for time-varying disturbances, ultimately contributing to improved observer stability and accuracy.

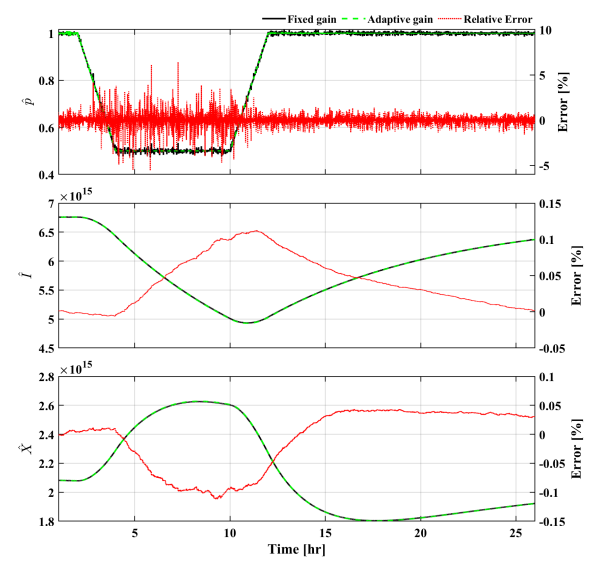


Figure 4. Estimated states using fixed and adaptive gain SMO

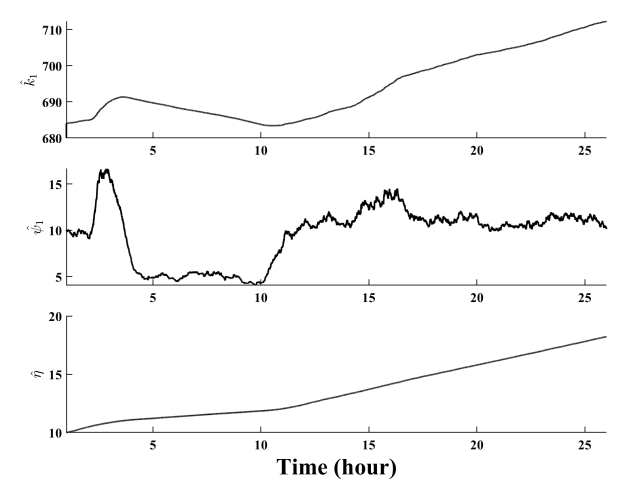


Figure 5. Adaptive gain trajectories during load-follow operation

5. Conclusions

In this study, we proposed an improved sliding mode observer for xenon estimation during daily load follow operation. By implementing the implicit Euler method in the sliding mode observer model, numerical chattering is effectively mitigated and the computational cost is greatly reduced compared to the explicit scheme. In addition, adaptive laws for observer and controller gain are introduced to enhance the robustness of the observer under perturbed measurement signals and varying power conditions. Simulation results based on the APR1400 core confirmed that the proposed observer provides stable and accurate estimation of power and xenon dynamics across different operating conditions. Future research will explore systematic approaches for determining gain parameters without prior knowledge of disturbances to further improve the adaptability.

Acknowledgements

This work was supported by the Innovative Small Modular Reactor Development Agency grant funded by the Korea Government RS-2024-00405419.

REFERENCES

[1] H. Khalefih and Y. Kim, "Xenon estimation during load-follow operation using sliding mode observer in APR1400 for predictive soluble boron control," *Arab. J. Sci. Eng.*, vol. 50, no. 9, pp. 3491–3503 (2025).

[2] T. Oh et al., Development and validation of multiphysics PWR core simulator KANT, Nucl. Eng. Technol., 55(6), 2230–2245 (2023)